Journal of Building Engineering 59 (2022) 105128

Contents lists available at ScienceDirect

Journal of Building Engineering

journal homepage: www.elsevier.com/locate/jobe

Rock wool-reinforced concrete: Physico-mechanical properties and predictive modelling

Zhen Shyong Yap [a], Nur Hafizah A. Khalid [a,*], Zaiton Haron [a], Wai Hoong Khu [b], Su Hoe Yeak [c], Mugahed Amran [d,e]

[a] Faculty of Civil Engineering, Universiti Teknologi Malaysia, 81310, Johor Bahru, Johor, Malaysia
[b] Faculty of Chemical and Energy Engineering, Universiti Teknologi Malaysia, 81310, Johor Bahru, Johor, Malaysia
[c] Department of Mathematical Sciences, Faculty of Science, Universiti Teknologi Malaysia, 81310, Johor Bahru, Johor, Malaysia
[d] Department of Civil Engineering, College of Engineering, Prince Sattam Bin Abdulaziz University, 16273, Alkharj, Saudi Arabia
[e] Department of Civil Engineering, Faculty of Engineering and IT, Amran University, 9677, Amran, Yemen

ARTICLE INFO

Keywords:
Rock wool fiber
Lightweight concrete
Mechanical properties
Physical properties
Prediction model

ABSTRACT

Recent developments in lightweight concrete (LWC) have led to a renewed interest in incorporating fibers in concrete. However, research on the specific application of rock wool fiber in LWC is scarce. Hence, the present study aims to investigate the physical and mechanical characteristics of LWC with the inclusion of rock wool fibers (0%–15%) in different water-cement ratios (0.4, 0.5 and 0.6). The relationships between mix proportion and the density, permeable void, water absorption, compressive strength, splitting tensile strength and flexural strength of the composite were investigated. The results showed the density of the rock wool-incorporated specimen was highly reduced (up to 73% reduction) when the incorporation of rock wool fiber reached 15%. The oven-dry densities of the specimens for fiber contents from 2.5% to 10% are 800 kg/m^3 to 2000 kg/m^3, which can be classified as LWC. Permeable voids of the specimens were increased by 63% by volume with 15% of rock wool inclusion. Only a certain mix proportion fulfilled the requirement to be used as load-bearing internal walls. The correlation between compressive strength and splitting tensile strength was subsequently analyzed. Lastly, the empirical models for all properties were generated using the response surface method with $R^2 > 0.90$. In conclusion, the selection of different mix ratios of rock wool and the water-cement ratio (w/c) for attaining better physical or mechanical properties of LWC will be presented, and hopefully serves as a sound basis for future related studies.

1. Introduction

In recent years, land resources in cities have become increasingly limited as the economy and society have developed rapidly. The number of high-rise buildings has increased dramatically, allowing additional living and development space [1,2]. In line with the soaring demand for high-rise buildings, researchers are focusing on investigating innovative lightweight concrete (LWC) materials [3,4]. The benefit of LWC is to reduce the material's self-imposed weight on the structure, which lowers reinforcement ratios and reduces the construction cost. A recent study proved that using LWC blocks as partition walls reduces the direct cost of an apartment by 8.2% to 13.9% [5]. Besides, LWC also found its potential in thermal insulation [6,7], sound insulation [8,9], seismic structural response [5] and

* Corresponding author.
E-mail address: nur_hafizah@utm.my (N.H. A. Khalid).

https://doi.org/10.1016/j.jobe.2022.105128
Received 18 June 2022; Received in revised form 26 July 2022; Accepted 11 August 2022
Available online 17 August 2022

energy-saving [10] applications. Extensive research has shown that incorporating LWC in a high-rise building can achieve 3.2%–14.8% of energy savings.

The average density of regular concrete is around 2400 kg/m^3. The British Standard European Norm (ACI) specifies the dry density of structural LWC ranges from 800 kg/m^3 to 2000 kg/m^3 [11]. The concrete below this weight range is considered non-structural and sometimes coined as ultra-lightweight or infra-lightweight concrete [12,13]. The density of concrete is well acknowledged to significantly impact and improve the specific properties of LWC such as sound insulation [14], thermal insulation and fire resistivity. As a result, more recently, there has been a surge of interest in incorporating different materials and investigating their influences on the density of LWC [15,16].

As of late, development in LWC has garnered the interest of many researchers, spurring them to incorporate different types of fibers (natural or synthetic) in concrete. Aside from density reduction, the use of natural fibers in LWC can help to reduce the carbon footprint and agricultural waste [17]. A recent review study has summarized the common natural fibers used in LWC, including oil palm waste [18], rice husk [19], crushed groundnut shell, olive waste, sugarcane waste, hemp, buckwheat husk, etc. [20]. Despite the numerous benefits described above, natural fibers have recurring biodegradation issues, including UV-induced degradation and breakdown of the structures that cement the fibers together cause by weak bonding. Pre-treatments are commonly used to fix these difficulties, but it is expensive and not environmentally sustainable [21–23]. Furthermore, a few studies have reported that the homogeneous qualities of natural fibers are difficult to control because they are highly dependent on field climate conditions. This can cause an undesired variation of fiber properties and subsequently leading to other quality problems down the road [24,25]. Overall, microbial activity and degradation are the major hindrances in using natural fiber in the concrete matrix [26,27].

One of the alternative materials is synthetic fiber. A previous review study has stated that numerous researchers were focusing on incorporating different synthetic fibers into LWC, such as basalt fiber, glass fiber, bagasse fiber, carpet fiber, polyvinyl alcohol fiber, polyethylene fiber, polypropylene fiber and tire wire fiber [28]. Synthetic fibers are widely regarded as superior than natural fibers in terms of heat and sound insulation [29]. Other than the above-mentioned synthetic fibers, one of the most popular synthetic fibers which has been extensively applied as an insulator material is rock wool. Rock wool is a product of molten rock at a temperature of around 1600 °C that is blown through with a stream of air. Basalt fibers and expanded or extruded polyurethane resins are used to create rock wool composites. For decades, rock wool fibers have been extensively applied as insulator materials due to their excellent heat and sound insulating properties, low densities, high tensile strengths, and most importantly, low costs [30]. For instance, several researchers have studied the incorporation of rock wool fibers into popular materials such as polyurethane foams [31,32] and aerogels [33,34]. Generally, the incorporation of rock wool fibers has improved the physical and thermal characteristics of said materials.

However, based on current literature, the application of rock wool fiber in LWC is relatively scarce. This study aims to bridge this knowledge gap through a thorough investigation on the physico-mechanical effects of incorporating rock wool fibers with the concrete matrix (a mixture of cement and water). The relationship between mix proportions and the density, permeable void, water absorption, compressive strength, splitting tensile strength and flexural strength of the final composite were investigated. The relationships between the compressive strength of the specimens and the weight ratio, as well as the splitting tensile strength, were analyzed respectively. Lastly, the empirical models for each property were identified using the response surface method.

2. Materials and methods

2.1. Materials

The lightweight material used in this study was rock wool, procured from local commercial sources and certified by MS 1020:2016 and BS EN 13501-1: 2007 +A1:2009. The bulk density of rock wool used in this study was 80 kg/m^3. The rock wool was cut into 2 cm^3 cubes as shown in Fig. 1(a), before mixing with the binder. The binder comprises of tap water and Ordinary Portland Cement, certified by MS EN 193-1:2004.

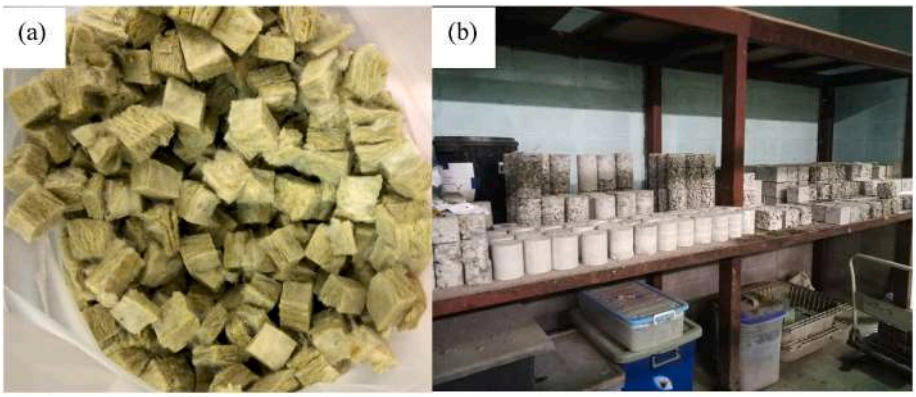

Fig. 1. (a). Rock wool in cubic shape; (b) air-dried curing environment.

2.2. Mix design

The mix formulation is shown in Table 1. The manipulating variables are rock wool-cement ratio (wt.%) and water-cement ratio (wt.%). The rock wool-cement ratios used were 0%, 2.5%, 5%, 7.5%, 10%, 12.5% and 15% with different water-cement ratios (w/c) 0.4, 0.5 and 0.6. During the investigation of the relationship between hardened concrete properties and water uptake, the amount of water is fixed, although the workability of fresh concrete might differ from one to another.

2.3. Specimens' preparation

The rock wool cubes were dry-mixed with cement for at least 120 s, followed by a slow addition of water and uniform mixing for an additional 120 s to ensure a homogeneous concrete matrix. After mixing, the fresh concrete was poured and layered into cubic ($100 \times 100 \times 100$ mm^3), prismatic ($75 \times 75 \times 300$ mm^3), and cylindrical (diameter 100 mm and height 200 mm) steel molds, for a total of three layers. Each layer of fresh concrete was subjected to mechanical vibration for 5 s on the vibrating table for compaction, and the process was repeated for the subsequent layer. The compacted specimens were covered with an impervious plastic sheet for 24 ± 8 h at the laboratory temperature ($26\ ^\circ\text{C} \pm 2\ ^\circ\text{C}$) to reduce the evaporation of water. Then, the specimens were unmolded and dry-cured in a vibration-free environment for more than 28 days before testing as shown in Fig. 1(b).

2.4. Experimental procedures

2.4.1. Bulk density

Bulk density is the fundamental parameter that must be determined to accurately predict the properties of the concrete block while also monitoring the consistency of the specimen's production. The triplicate cubic samples ($100 \times 100 \times 100$ mm^3) for each mix were tested at the age of 28 days. The specimens were dried in the oven at a temperature of $110 \pm 5\ ^\circ\text{C}$ for 72 h to acquire the oven-dry mass. The density was then measured according to the appropriate ASTM standards [35].

2.4.2. Permeable void ratio and water absorption

The permeable void ratio and the degree of water-tightness of the porous concrete specimens were determined in accordance to the modified ASTM standards [36] by drying and subsequently immersing said specimens in water. 63 cubic specimens (in triplicates) with a length of 100 mm were cured for 28 days before the test. Three key parameters were measured in order to determine the permeable void ratio and the percentage of water absorption, namely the oven-dried mass of the specimen, the saturated-surface-dry mass of the specimen, and the apparent mass when the specimen is submerged. The procedures for determining the oven-dried mass were the same as the previous section. To obtain the apparent mass during submersion, the specimens were placed in the water for more than 24 h and their masses were subsequently measured while being submerged. The specimens were removed from water and the surface was dried immediately to obtain the surface-saturated-dry mass of each specimen. Using these parameters, the calculations of the percentage absorption and the permeable void ratio were shown as follows.

$$\text{Absorption after immersion, } \% = [(B - A)/A] \text{ x } 100 \tag{1}$$

$$\text{Permeable pore space (voids) ratio, } \% = [(B–A)/(B–C)] \text{ x } 100 \tag{2}$$

where:

A = mass of oven-dried sample in air, g
B = mass of surface-dry sample in the air after immersion, g
C = apparent mass of sample in water after 24-h immersion, g

2.4.3. Compressive strength

This test aims to determine the compressive strength of hardened concrete [37] to ensure the material meets the specific structural requirements. The cubic specimen triplicates ($100 \times 100 \times 100$ mm^3) for each mix were tested at the age of 28 days. The specimens were positioned in the Universal testing machine so that the load was applied perpendicularly to the direction of casting. The testing

Table 1
Mix proportion of rock wool concrete.

Notation	Rock Wool to Cement (wt%)	Water-Cement-Ratio (wt%)	Notation	Rock Wool to Cement (wt%)	Water-Cement-Ratio (wt%)
R0W4	0.0	0.4	R10W4	10.0	0.4
R0W5		0.5	R10W5		0.5
R0W6		0.6	R10W6		0.6
R2.5W4	2.5	0.4	R12.5W4	12.5	0.4
R2.5W5		0.5	R12.5W5		0.5
R2.5W6		0.6	R12.5W6		0.6
R5W4	5.0	0.4	R15W4	15.0	0.4
R5W5		0.5	R15W5		0.5
R5W6		0.6	R15W6		0.6
R7.5W4	7.5	0.4			
R7.5W5		0.5			
R7.5W6		0.6			

machine, with a capacity of 200 kN, applied a loading rate of 6 kN/s to the specimens until failure was reached. The compressive strength of the specimen was subsequently calculated according to Eq. (3). The average of the compressive strength values of the triplicates was obtained as the final compressive strength for a particular mix design.

$$f_c = (F / A_c) \times 100 \tag{3}$$

where:

f_c = compressive strength, MPa;
F = maximum load at failure, N;
A_c = cross-sectional area of the specimen on which the compressive force acts, mm^2

2.4.4. Splitting tensile strength

Cylindrical specimen triplicates (200 mm height and 100 mm diameter) for each mix were subjected to splitting tensile strength testing in accordance to the appropriate ASTM standards [38] at the age of 28 days. The specimens were placed in the testing machine and aligned to the center. Thin, plywood bearing strips were used to distribute the load applied along the length of the cylinder. A loading rate of 0.04 MPa/s was applied continuously on the specimens without any shock until failure was reached. The maximum load applied to the specimens was recorded. The splitting tensile strengths were then calculated as follows:

$$f_t = 2P/\pi/\mathrm{d} \tag{4}$$

where:

f_t = splitting tensile strength, MPa;
P = maximum applied load indicated by the testing machine, N

2.4.5. Flexural strength

The flexural test in this study was carried out strictly according to the specific standards [39]. A flexural test machine with two-point loading was used in this test. Specimens were placed in the flexural test machine without shock, and the loading rollers were lowered down until they were in contact with the test specimen. A 0.04 MPa/s loading rate was applied to the specimen until failure occurred and the maximum load values were recorded. The flexural strength can be calculated using the equation below:

$$f_f = FL/(bd^2) \tag{5}$$

where:

f_f = flexural strength, MPa;
F = maximum load, N;
L = distance between the supporting rollers, mm;
b = width of the test specimen, mm;
d = thickness of test specimen, mm.

2.5. Predictive regression models

A three-level factorial experimental design with 5 replicates at the center point, and a set of points lying at the midpoint of each

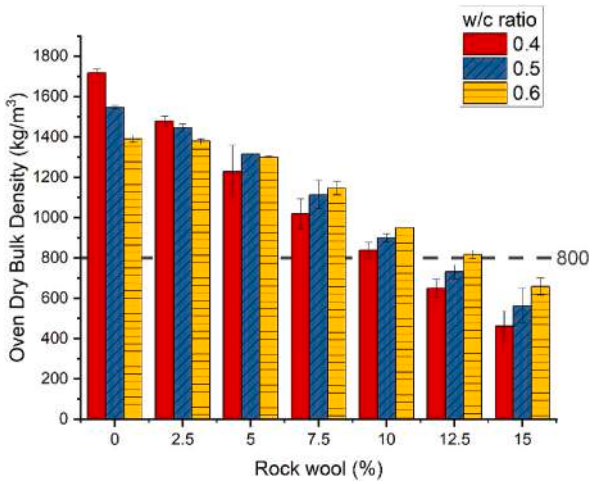

Fig. 2. Density against w/c ratio and rock wool content.

edge of the multidimensional cube that defines the region of interest was used. The processing variables (rock wool and w/c ratio) and predictive regression models were constructed for density, permeable void, water absorption, compressive strength, splitting tensile strength and flexural strength. The experimental design involved 21 runs where all checkpoints were performed over the entire experimental domain to validate the chosen experimental design and polynomial equations. The response surface analysis was performed using Design Expert Version 6.0 software, where 3D response surface plots were drawn for each model.

3. Results

3.1. Density

The oven-dry bulk density for each specimen was measured to predict the properties of the concrete while monitoring the consistency of the specimen's production. Fig. 2 depicts the trends for the influence of rock wool ratio and w/c ratio on oven-dry density. Generally, all the figures show a decreasing trend in bulk density by increasing rock wool proportion. These results could be explained by the addition of rock wool significantly generating the pores between the hardened paste. Thus, the overall bulk densities were significantly reduced.

A closer inspection of the figure shows little difference in water-cement ratio to the decreasing rate of bulk density. The mixtures with a 0.4 w/c ratio show approximately 73% reduction after incorporating 15% of rock wool, while mixtures with 0.5 and 0.6 w/c ratios dropped 64% and 53%, respectively. In other words, with the increasing of rock wool fiber content, additional water is needed to maintain the density of the concrete. The differences may be attributed to the water absorption competition between binder and rock wool during the mixing process. Also, the water absorbed by rock wool was partially dried out from the open continuity pores, leading to a decrease in oven-dry bulk density. This result aligns with previous findings on LWC [4,40,41]. Hence, a higher w/c ratio is needed to avoid water absorption competition between rock wool and the binder for higher rock wool content.

Through predictive regression, a density model has been generated empirically in the form of Eq. (6). The Model F-value of 415.19 implied that this model is significant and there is only a 0.01% chance that a "Model F-value" this large could occur due to noise, thus implying that it is a well-fitted model. In addition, the values of "Prob > F" are less than 0.0001, indicating model terms are significant. The aforementioned empirical density model expressed in terms of all the factors in this research is presented as follows, with the notation Rw being rock wool and W being water:

$$Density = 2075.85 - 974.98(W) - 144.76(Rw) + 153.57(W)(Rw) \quad (6)$$

A predicted against actual data was plotted in Fig. 3(a). The R^2 of 0.9865 indicated that this model was desirably fitted and adequately explained the data. The ratio of adequate precision of 63.766 was greater than 4, indicating adequate model discrimination. Overall, the 3D response surface was plotted as shown in Fig. 3(b), and this empirical model can be used to navigate the future experimental design space.

Overall, the oven-dry density for fiber content from 2.5% to 10% is in the range of 800 kg/m^3 to 2000 kg/m^3, which can be classified as LWC according to the standard guide stated in British Standard [11]. However, a closer look at the concrete with rock wool content >12.5% shows that it has less than 800 kg/m^3, and is thus considered as ultra-lightweight concrete. As lightweight concrete or ultra-lightweight material is in demand in high-rise buildings nowadays [5,42], incorporating rock wool into concrete is a potential alternative LWC to the future development of construction materials.

3.2. Permeable void volume

Fig. 4 shows the trend of the permeable void in the specimens with different rock wool fiber content and w/c ratio. It is hypothesized that the volume of permeable voids increases as the rock wool content increases due to the high porosity property of rock wool fiber. This finding is in agreement with previous fiber reinforcement concrete studies [43].

A closer look in the figure shows that the impact of the w/c ratio on the permeable void content depends on the amount of rock wool fiber. For instance, at 0% and 2.5% of rock wool content, when the w/c ratio increases from 0.4 to 0.6, the volumes of permeable voids increase 63% and 35%, respectively. It is understood that when only a small amount of rock wool is added into the mixtures, the

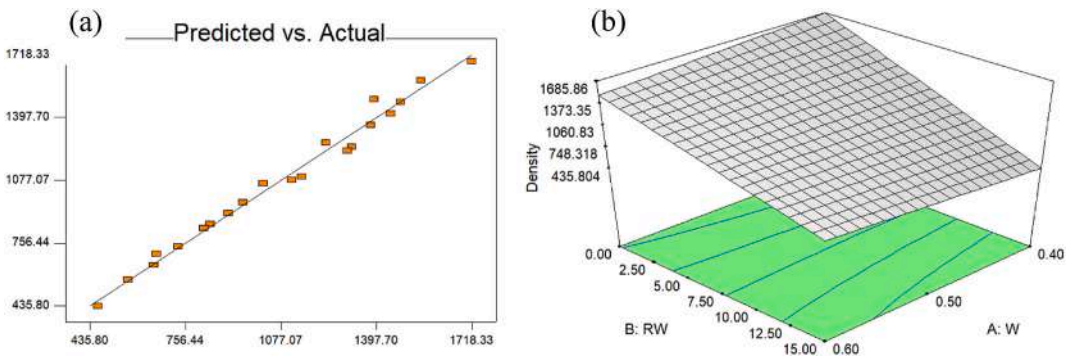

Fig. 3. (a). Predicted density against actual density (b) 3D response surface for density based on the empirical prediction model.

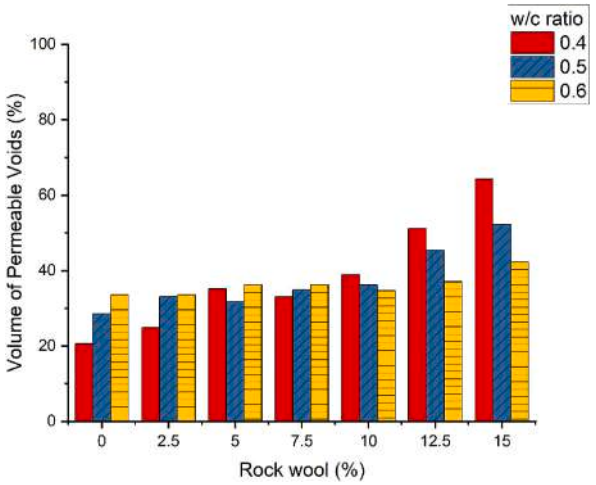

Fig. 4. The volume of permeable voids against w/c ratio and rock wool content.

cement paste becomes the major component. Hence the relationships may be primarily explained from the cement paste. When more w/c ratio was added to the mixture, the excess water in the cement paste was not consumed by the hydration reaction, causing extremely small pores between the gel after hardening. This indicated that for a low amount of rock wool, the more water is added, the more permeable pores are formed in the medium.

Interestingly, when the rock wool amount exceeded 10%, the increase in w/c ratio had the opposite effect on the permeable voids volume. For example, at 10%, 12.5% and 15% of rock wool (Fig. 4), when the w/c ratio increased from 0.4 to 0.6, the permeable voids volume decreased by 11%, 28% and 34%, respectively. The voids volume declined when the w/c ratio increased because when more water is added into the mixtures, the high workability of the cement paste is more easily filled into the empty spaces of the rock wool, causing lower porosity in the general mixtures. A previous study also recorded a similar observation [44].

A predictive regression model for the permeable void was generated empirically in the form of Eq. (7). The Model F-value of 48.8 implied that this model is significant and there is only a 0.01% chance that a "Model F-value" this large could occur due to noise, showing that it is a well-fitted model. In addition, values of "Prob > F" are less than 0.0001, indicating that the model terms are significant. The final empirical model for the permeable void in term of various factors is presented as follows:

$$PermeableVoids = -12.64 + 93.40(W) + 5.66(Rw) - 20(W)^2 + 0.10(Rw)^2 - 11.16(W)(Rw) \quad (7)$$

A predicted against actual data was plotted in Fig. 5(a). The R^2 of 0.9413 indicated that this model was desirably fitted and adequately explained the data. The ratio of adequate precision of 27.379 was greater than 4, indicating adequate model discrimination. Overall, the 3D response surface was plotted as shown in Fig. 5(b), and this empirical model can be used to navigate the future experimental design space.

3.3. Water absorption

This section examines the impact of varying rock wool fiber contents in concrete on the water absorption of the specimens. Water absorption was determined according to the ASTM-C20 standard. The trend depicts an increase of water absorption percentage when fiber content increases (Fig. 6). The trend in water absorption of concrete can likely be attributed to the resulting void volume. In particular, in specimens with a large void percentage, water absorption was higher. This performance is in alignment with the

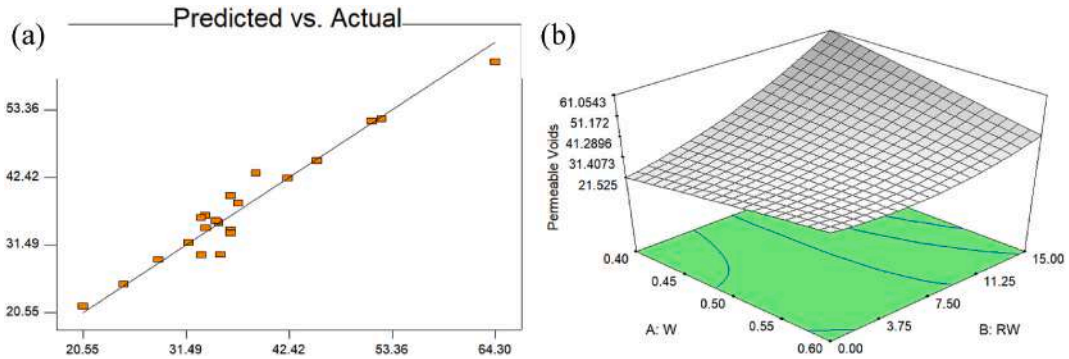

Fig. 5. (a). Predicted permeable void against actual permeable void (b) 3D response surface for permeable void based on the empirical prediction model.

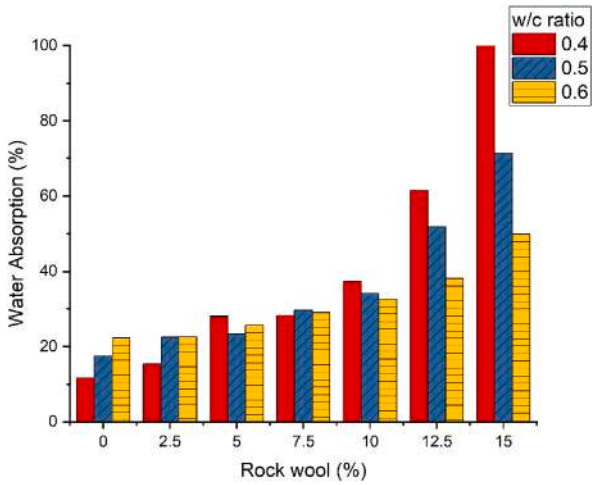

Fig. 6. Water absorption against w/c ratio and rock wool content.

outcomes of a similar fiber-incorporated concrete study [43].

One interesting finding is that the impact of the w/c ratio on the water absorption is in contrast with the impact of varying rock wool content. For an instant, 0% and 2.5% of rock wool, as the w/c ratio increases, the water absorption capacity increases. This increase is due to the presence of too much water in the hydration reaction that causes massive small gel pores in the hardened cement paste. As mentioned in the literature review, those gel pores are called capillary pores, mainly within the size range 0.01–10 μm, resulting in the permeability and diffusivity of the concrete [45]. One unexpected finding was the extent to which the w/c ratio shows a different set of results in water absorption for more than 10% of rock wool content (see Fig. 6). This result is similar to that observed in the permeable voids volume section. As previously mentioned, a higher w/c ratio provokes higher workability of hydration products which may occupy the inner space of rock wool. Thus the overall voids decreased. In addition, the high absorptive properties of rock wool may cause an excessive absorption of water and lead to insufficient water for the hydration reaction, resulting in more pores in between the hydrated gel. Hence, the lower w/c ratio of the mixtures shows a higher water absorption at that point. Overall, lower water absorption is expected at a higher w/c ratio, or vice versa, owing to the permeable voids volume.

To develop an empirical model for water absorption, predictive regression was used once again. The empirical model was generated in the form of Eq. (8). The Model F-value of 89.57 implied that this model is significant and only a 0.01% chance that a "Model F-value" this large could occur due to noise, showing that it was a well-fitted model. In addition, values of "Prob > F" are less than 0.0001, indicating model terms are significant. The final empirical water absorption model in term of all factors is presented as follows:

$$WaterAbsorption = -40.75 + 167.41(W) + 6.60(Rw) - 93.43(W)^2 + 0.25(Rw)^2 - 14.35(W)(Rw) \quad (8)$$

A predicted against actual data was plotted in Fig. 7(a). The R^2 of 0.9676 indicated that this model was desirably fitted and adequately explained the collected data. The ratio of adequate precision of 33.173 was greater than 4, indicating adequate model discrimination. Overall, the 3D response surface was plotted as shown in Fig. 7(b), and this empirical model can be used to navigate the future experimental design space.

Overall, although the water absorption cannot be used as a measure of the quality of the porous concrete, the result suggests that when rock wool or other high water absorptive fiber are being introduced in batches, the amount of water added to the plant must be

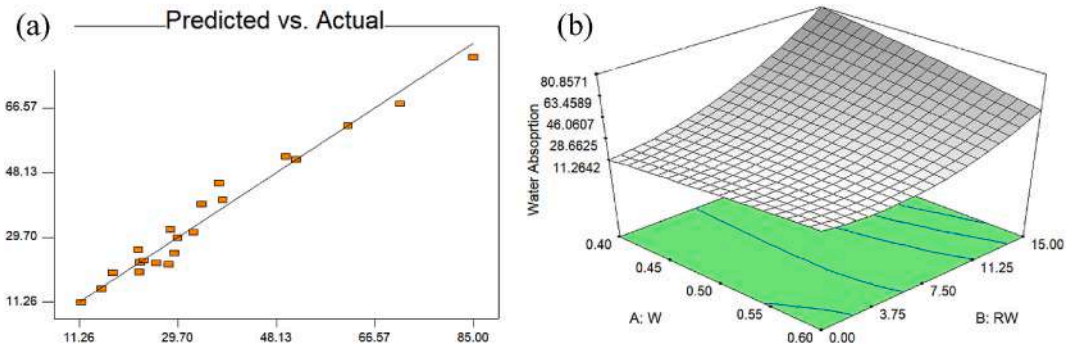

Fig. 7. (a). Predicted water absorption against actual water absorption (b) 3D response surface for water absorption based on the empirical prediction model.

increased to maintain the desired porosity and water absorption properties. According to recent literature findings and perspectives [46–48], high water-absorbing materials like rock wool has the potential to be used as an internal curing agent. The pre-wet rock wool can act as a reservoir that slowly releases moisture to cementitious hydration reaction in the pores to improve shrinkage issues in high-strength concrete [49].

3.4. Compressive strength

Despite LWC possessing many advantages, it is substantially more fragile than traditional concrete, and it is imperative to find the optimum rock wool content and w/c ratios that yield LWC batches with strength being comparative to that of typical concrete. Hence, this study investigates the variation of compressive strength with different rock wool ratios and w/c ratios. For R10W4, R12.5W4, R15W4, R12.5W5, R15W5 and R15W6, the compressive strength values were below the measurable range of the machine, hence they are not shown in Fig. 8. As depicted in the figure, the compressive strength decreases dramatically as the rock wool ratio increases. The negative influence of non-structural fibers on compressive strength is often found in literature as well [40,50,51]. The decrease in compressive strength is mainly due to two possible reasons: (i) the increased rock wool content lowers the binder's ratio in the fixed mixture's volume, leading to many intergranular voids. The compressive strength depends on the hardened binder surrounding the rock wool fibers, which affects the proper load distribution, and (ii) the high water absorptive properties of the rock wool inclusions will hinder the formation of the hydration products in the paste and lead to a decrement in mechanical strength. As a summary, incorporating rock wool fiber in the matrix could lead to perforations and subsequent internal flaws in interfacial transition zones and thus reduce the compressive strength. Similar findings were found in previous studies [52,53]. For instance, one of the recent studies revealed 88.9% of strength degradation after adding 1.5 wt% of polypropylene fiber into the concrete matrix [54].

It is apparent from this Fig. 8 that there was a slight difference in compressive strength results with different w/c ratios. The lower w/c ratio in the LWC decreases more significantly with increases in rock wool content. For instance, 0.4 w/c ratio yielded a strength decrease by 93.6% after adding 5% of rock wool fiber, while 0.5 w/c ratio & 0.6 w/c ratio have resulted in a drop of 83.6% and 80.6%, respectively. This could be due to the adsorption of water by the rock wool fiber in the freshly mixed material (high water absorption rate found in high open-end pores of rock wool), thereby not leaving sufficient water for the hydration reaction of the lime. The incomplete hydration process would prevent the lime from reaching its maximum potential strength. In summary, different w/c ratios play a crucial role in attaining the desired compressive strength. A lower w/c ratio has a significant negative effect on compressive strength as the fiber content increases. Therefore, when the volume of fiber increases, a higher w/c ratio is needed to avoid the incomplete hydration of lime, which will negatively affect the concrete strength.

A predictive regression model for compressive strength has been generated empirically in the form of Eq. (9). The Model F-value of 27.22 implied that this model is significant and there is only a 0.01% chance that a "Model F-value" this large could occur due to noise showing it was a well-fitted model. In addition, the values of "Prob > F" are less than 0.0001, indicating that the model terms are significant. The final empirical compressive strength model in terms of all factors is presented as follows:

$$CompressiveStrength = 75.50 - 74.26(W) - 11.23(Rw) + 0.86(W)^2 + 0.35(Rw)^2 + 7.17(W)(Rw) \quad (9)$$

A predicted against actual data was plotted in Fig. 9(a). The R^2 of 0.9007 indicated that this model was desirably fitted and adequately explained the collected data. The ratio of adequate precision of 16.315 was greater than 4, indicating adequate model discrimination. Overall, the 3D response surface was plotted as shown in Fig. 9(b), and this empirical model can be used to navigate the future experimental design space.

Overall, the determination of the compressive strength of hardened specimens ensures the material meets the specific strength requirements. According to LWC standard [55], the concrete produced with a combination of normal weight and lightweight

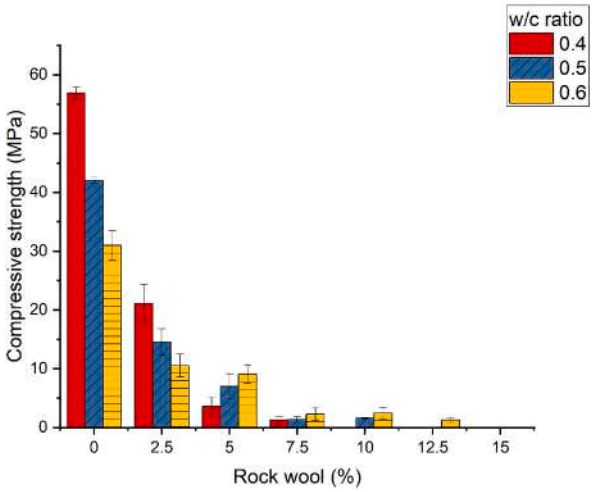

Fig. 8. Compressive strength against w/c ratio and rock wool content.

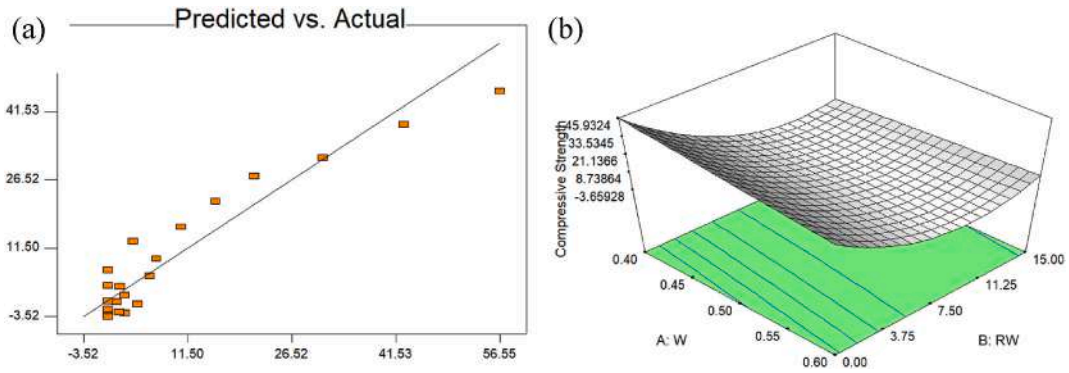

Fig. 9. (a). Predicted compressive strength against actual compressive strength (b) 3D response surface for compressive strength based on the empirical prediction model.

aggregates shall conform to a minimum compressive strength of 17 MPa and a maximum density of 1,680 kg/m^3 to be considered as a structural LWC. Only R2.5W4 meets the requirement. R2.5W5 and R2.5W6 fulfilled the Class 1 and Class 2 load-bearing block requirements respectively, according to Standard [56] whereas R5W4, R5W5, R5W6, R7.5W6 and R10W6 fulfilled the requirement to be used as load-bearing internal walls block with not less than 2.8 MPa compressive strength. In conclusion, despite the rock wool composite concrete being extremely low in compressive strength, it is still sufficient to use them for non-structural applications for less than 5 wt% of fiber content.

3.5. *Splitting tensile strength*

It is crucial to determine the capacity of LWC to resist cracking or breaking under tension. Numerous studies have investigated the mixing of fiber in the cementitious matrix to improve the tensile strength of concrete. However, rock wool fiber did not yield a desirable result in this study. Fig. 10 depicts the splitting tensile strengths for three different w/c ratios. The values for samples with 0.4 w/c ratio dropped dramatically from 0% to 15% of rock wool, followed by samples with 0.5 w/c ratio and 0.6 w/c ratio. Samples R12.5W4, R12.5W5, R15W4, R15W5 and R15W6 have failed to produce conclusive results due to the limitation of the machine on lower strength specimens. The strength degradations may be caused by the generation of voids as mentioned in the previous section and the agglomeration of rock wool, resulting in the non-uniform distribution of stresses and inferior performance as a whole. Although most of the fiber-reinforced cementitious composite studies exhibited excellent dynamic mechanical properties in splitting tensile strength [51,57,58], there are some studies which reported a degradation of strength after fiber incorporation. For instance, in a recent study, the recorded splitting tensile strength with 1.5% of polypropylene fiber content was 0.92 MPa [54], which was a 68.8% decrease from the control specimen. Another study revealed that the addition of fiber does not produce a clear conclusive effect on the variation in splitting tensile strength [57]. The inconsistent tensile strength results of fiber inclusion in concrete can be attributed to the unpredictable tensile strength of fiber as well as the diameter ratio of the fibers [59] and its bonding strength with the matrix [58,60], as most fiber sources consist of non-homogeneous fibers with different properties.

The rock wool concrete in this study was compared with other LWC findings. A comparison graph on splitting tensile strengths from

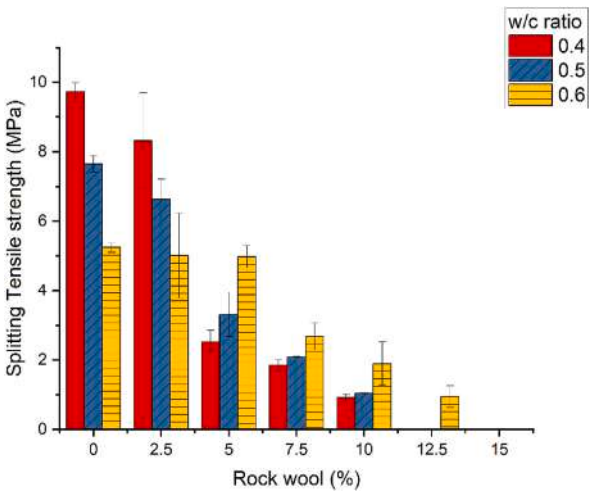

Fig. 10. Splitting tensile strength against w/c ratio and rock wool content.

different academic sources was plotted against the compressive strength (Fig. 11). The predictions on splitting tensile strengths were made based on the LWC mathematical models (Table 2), and a comparison was made between the experimental and predicted data. Other than the standard equation proposed by the American Concrete Institute [61], a few more equations were proposed by previous LWC studies, including models for foam concrete [62], lightweight aggregates concrete [63–65] and fiber-incorporated concrete [66].

Evidently, the experimental data were distributed above all the predicted data points (Fig. 11). In other words, none of the equations in previous LWC studies can accurately estimate the splitting tensile strength of rock wool concrete. Therefore, a novel empirical equation was proposed for rock wool concrete, as shown in Eq. (10). Single regression analysis is performed on the figure to identify the correlation of the equation to the experimental results. $R^2 = 0.88$ was obtained, which explains this equation was fitted to the actual data adequately.

$$f_t = -20.33 + 20.77\, f_c^{0.085} \tag{10}$$

The proposed equation is a powerful model in line with most of the previous LWC studies in Table 2. Some studies showed a linear relationship [66]. A simpler directly-proportional relationship was proposed by a review study [67], which reported that the splitting tensile strength of LWC ranges from 15% to 35% of its compressive strength. Such variations may be attributed to the fact that the determination of tensile strength is more sensitive to the test conditions than that of compressive strength.

To develop an empirical model for splitting tensile strength in the form of Eq. (11), predictive regression was used once again. The Model F-value of 34.60 implied that this model is significant and there is only a 0.01% chance that a "Model F-value" this large could occur due to the noise, showing that it is a well-fitted model. In addition, the value of "Prob > F" is less than 0.0001, indicating that the model terms are significant. The final splitting tensile strength empirical model in terms of all factors is presented as follows:

$$SplittingTensileStrength = 18.67 - 30.04(W) - 1.70(Rw) + 16.79(W)^2 + 0.03(Rw)^2 + 1.49(W)(Rw) \tag{11}$$

A predicted against actual data was plotted as shown in Fig. 12(a). The R^2 of 0.9202 indicated that this model was desirably fitted and adequately explained the collected data. The ratio of adequate precision of 19.566 was greater than 4, indicating adequate model discrimination. Overall, the 3D response surface was plotted as shown in Fig. 12 (b), and this empirical model can be used to navigate the future experimental design space.

In whole, the presence of fibers yielded a degradation of the splitting tensile strength, which is similar to the observations in the previous compressive strength study. It can be concluded that the compressive strength factors also affect the tensile strength and vice versa. The improvement in strength development of tensile strength shared a similar trend and displayed a power model relationship with the compressive strength development. One of the potential solutions proposed by the previous study to address the degradation in splitting tensile strength is to reinforce the fly ash-based geopolymer in the matrix [68]. Nevertheless, more studies concerning the tensile strength of rock wool-incorporated LWC is essential in order to better grasp and assess the feasibility to fully substitute conventional concrete with rock wool LWC in major structures.

3.6. Flexural strength

After reviewing compressive and splitting tensile strengths, this section is aimed toward flexural strength, which also displayed a similar trend. Fig. 13 shows the influence of rock wool fiber content on flexural strength with different w/c ratios. Some of the specimens with 10% and above fiber content were below the measurable range of the machine and hence, were excluded from the figure. Flexural strength decreases dramatically with increasing fiber for all different w/c ratios (0.4, 0.5 and 0.6). The results indicated that the flexural strength values depend on the fiber content but were less controlled by the w/c ratio. One of the potential factors which causes the degradation of flexural strength is that the incorporation of rock wool reduces the solid content in the overall matrix. To be more precise, when rock wool was being incorporated up to a certain limit, the binder volume relatively decreased as the total

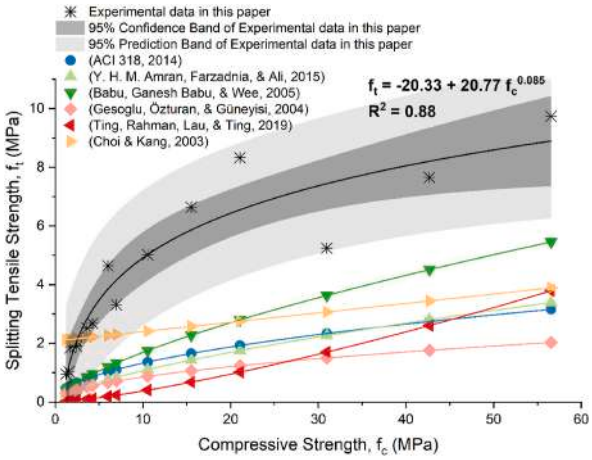

Fig. 11. Splitting tensile strength against compressive strength.

Table 2
Presents empirical equations developed by previous LWC on splitting tensile strength (f_t) against compressive strength (f_c).

Equation	Annotations	References
$f_t = 0.56\ \lambda\ (f_c)^{0.5}$	$\lambda = 0.75$ for LWC	[61]
$f_t = 0.23\ (f_c)^{2/3}$	Foam concrete	[62]
$f_t = 0.358\ (f_c)^{0.675}$	Expanded polystyrene	[63]
$f_t = 0.27\ (f_c)^{0.5}$	Fly ash aggregates	[64]
$f_t = 0.0177\ (f_c)^{1.33}$	Expanded shale	[65]
$f_t = 2.08 + 0.032\ (f_c)$	Glass fiber & polypropylene fiber	[66]

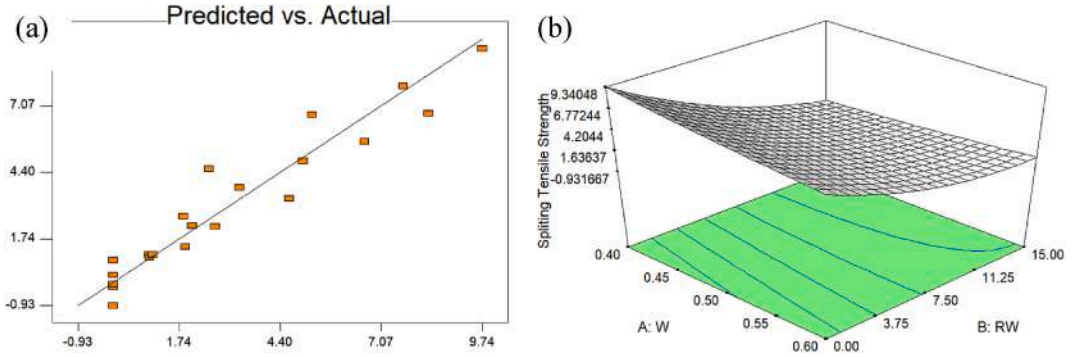

Fig. 12. (a). Predicted splitting tensile strength against actual splitting tensile strength (b) 3D response surface for splitting tensile strength based on the empirical prediction model.

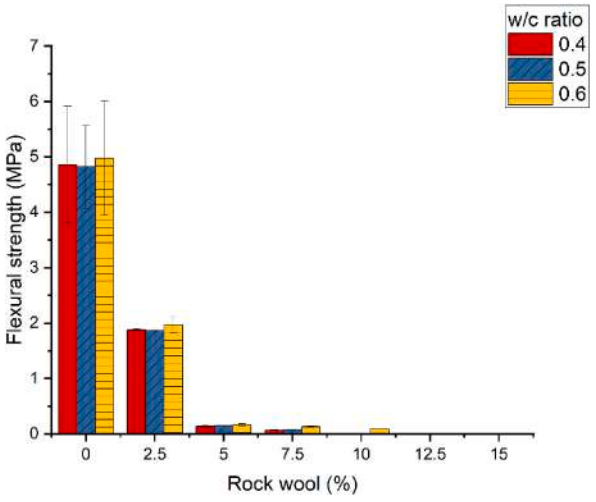

Fig. 13. Flexural strength against w/c ratio and rock wool content.

volume remained fixed, which caused an insufficient amount of binder to fill up the pores of the rock wool, which in turn resulted in a high porosity of rock wool fiber in the matrix space, significantly reducing the concrete density, and by extension, the bending/flexural strength. This result is in agreement with previous studies [60].

It is interesting to note that previous studies produced inconsistent findings on the flexural strength with similar fiber inclusions into the concrete matrix. For instance, one of the studies showed a 55.8% decrease in mechanical strength to 2.8 MPa after incorporating 1.5% of polypropylene fiber [54] whereas another study showed a 53% increase up to 8.9 MPa after incorporating 0.4% of glass fiber [51]. Although both studies used flexible and crunchable fibers similar to rock wool fiber, they reported very different changes in flexural strengths. This may be due to the different properties of fiber, such as the fracture toughness or tensile strength [28] and the bonding strength between the fibers and cement paste [69].

A predictive regression model for flexural strength was generated empirically in the form of Eq. (12). The Model F-value of 38.36 implied that this model is significant and there is only a 0.01% chance that a "Model F-value" this large could occur due to noise, thus suggesting that it was a well-fitted model. In addition, the value of "Prob > F" is less than 0.0001, indicating that the model terms are

significant. The final empirical model for flexural strength in terms of all factors in this study is presented as follows:

$$FlexuralStrength = 4.93 - 2.74(W) - 0.92(Rw) + 3.29(W)^2 + 0.4(Rw)^2 - 0.04(W)(Rw) \quad (12)$$

A predicted against actual data was plotted in Fig. 14 (a). The R^2 of 0.9275 indicated that this model was desirably fitted and adequately explained the data. The ratio of adequate precision of 19.566 was greater than 4, indicating adequate model discrimination. Overall, the 3D response surface was plotted as shown in Fig. 14 (b), and this empirical model can be used to navigate the future experimental design space.

4. Conclusions

This study investigated the variation in multiple physico-mechanical properties of LWC made with rock wool, cement, water in two proportions: rock wool (0%–15%) and w/c ratio (0.4 to 0.6). The physical and mechanical properties were measured for 21 specimens with different mix proportions and were subsequently evaluated. The properties being measured were density, porosity, water absorption, compressive strength, splitting tensile strength, and flexural strength. Empirical models for each property were proposed with a general desirable fit ($R^2 > 0.90$) based on the measurement results. The overall conclusions were drawn and enumerated as follows:

(a) The rock wool inclusions have a negative effect on bulk density. For fiber content between 2.5% and 10%, the oven-dry bulk density is 800 kg/m^3 to 2000 kg/m^3, which can be classified as LWC.
(b) At a lower w/c ratio (0.4), the permeable voids volume increases dramatically (up to 213%) as the rock wool content increases from 0% to 15%. On the other hand, at a higher w/c ratio (0.6), the increase of rock wool content does not contribute much on the permeable voids volume (up to 26%).
(c) From 0% to 2.5% of rock wool, as the w/c ratio increases, the water absorption capacity increases. Lower water absorption is expected at a higher w/c ratio, owing to the higher permeable voids volume.
(d) Overall, the compressive strength has a negative correlation with rock wool content regardless of different w/c ratios. Only mixtures with (i) < 5% of rock wool content with w/c ratio of 0.4, (ii) < 7.5% of rock wool content with w/c ratio of 0.5, and (iii) < 10% of rock wool content with w/c ratio of 0.6 fulfilled the requirement to be used as load-bearing internal wall blocks with at least 2.8 MPa compressive strength.
(e) Similar to the compressive strength observations, incorporating and increasing rock wool content in the specimens resulted in a dramatic drop in splitting tensile strength across different w/c ratios. Nevertheless, when compared to the splitting tensile strength against compressive strength ratios of other LWCs from past studies, the rock wool-incorporated concrete specimens in this study still showed an overall better tensile strength over the aforementioned LWCs.
(f) Overall, the flexural strength of rock wool-incorporated concrete has a similarly negative correlation with the rock wool content. In this case, the flexural strength of the specimens showed a strong dependence on the rock wool content but not on the w/c ratios, thus implying that the w/c ratio has little effect on the specimen flexural strength.

In conclusion, the selection of different mix ratios of rock wool and w/c ratio for attaining better physical or mechanical properties of LWC was commended in this study, which could be beneficial for future research and development. Further research may be needed to investigate the effects of fiber size and fiber distribution on different characteristics such as morphology, pore size, sound insulation and thermal insulation of LWC, thus providing a more holistic and comprehensive research and improving the understanding of the properties of rock wool-fiber-incorporated LWC as a whole.

CRediT authorship contribution statement

Zhen Shyong Yap: Conceptualization, Formal analysis, Writing – original draft, preparation, Visualization. **Nur Hafizah A. Khalid:** Supervision, Funding acquisition, Writing – review & editing. **Zaiton Haron:** Supervision, Writing – review & editing. **Wai Hoong Khu:** Writing – review & editing. **Su Hoe Yeak:** Supervision, Writing – review & editing. **Mugahed Amran:** Writing – review &

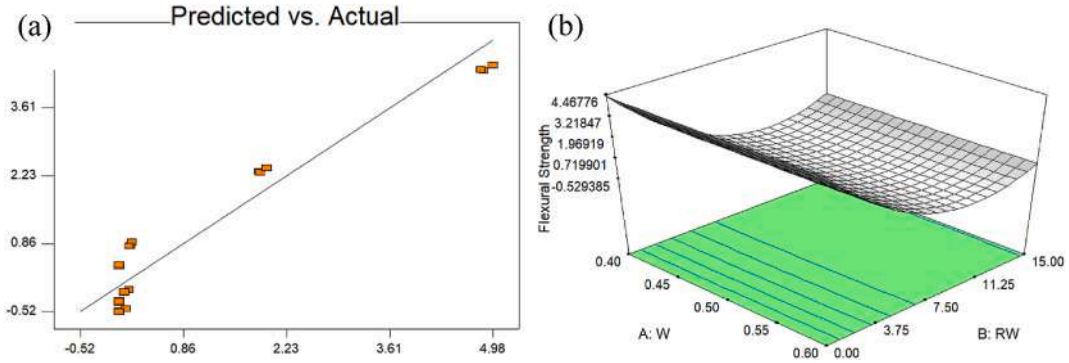

Fig. 14. (a). Predicted flexural strength against actual flexural strength (b) 3D response surface for flexural strength based on the empirical prediction model.

editing.

Declaration of competing interest

The authors declare that they have no known competing financial interests or personal relationships that could have appeared to influence the work reported in this paper.

Data availability

No data was used for the research described in the article.

Acknowledgements

The corresponding author is grateful to the Ministry of High Education and Universiti Teknologi Malaysia for the financial support under the research grant R.J130000.7851.5F034 (FRGS/1/2018/TK06/UTM/02/4) and Q.J130000.2451.09G91, respectively.

References

[1] B. Manzoor, I. Othman, A. Waheed, Accidental safety factors and prevention techniques for high-rise building projects – a review, Ain Shams Eng. J. 13 (2022), 101723, https://doi.org/10.1016/j.asej.2022.101723.
[2] B. Liu, D. Zhang, X. Li, J. Li, Tunnelling and Underground Space Technology incorporating Trenchless Technology Research Seismic response of underground structure – soil – aboveground structure coupling system : current status and future prospects, in: Tunnelling and Underground Space Technology Incorporating Trenchless Technology Research 122, 2022, 104372, https://doi.org/10.1016/j.tust.2022.104372.
[3] H.M. Hamada, A.A. Alattar, F.M. Yahaya, K. Muthusamy, B.A. Tayeh, Mechanical properties of semi-lightweight concrete containing nano-palm oil clinker powder, Phys. Chem. Earth 121 (2021), 102977, https://doi.org/10.1016/j.pce.2021.102977.
[4] B.A. Tayeh, A. Hakamy, M. Amin, A.M. Zeyad, I.S. Agwa, Effect of air agent on mechanical properties and microstructure of lightweight geopolymer concrete under high temperature, Case Stud. Constr. Mater. 16 (2022), e00951, https://doi.org/10.1016/j.cscm.2022.e00951.
[5] J. Strzałkowski, P. Sikora, S.Y. Chung, M. Abd Elrahman, Thermal performance of building envelopes with structural layers of the same density: Lightweight aggregate concrete versus foamed concrete, Build. Environ. (2021) 196, https://doi.org/10.1016/j.buildenv.2021.107799.
[6] M. Sadegh, T. Masoule, N. Bahrami, M. Karimzadeh, Lightweight geopolymer concrete : a critical review on the feasibility , mixture design , durability properties , and microstructure, Ceram. Int. 48 (2022) 10347–10371, https://doi.org/10.1016/j.ceramint.2022.01.298.
[7] H. Zhang, J. Yang, H. Wu, P. Fu, Y. Liu, W. Yang, Dynamic thermal performance of ultra-light and thermal-insulative aerogel foamed concrete for building energy e ffi ciency, Sol. Energy 204 (2020) 569–576, https://doi.org/10.1016/j.solener.2020.04.092.
[8] N. Flores Medina, D. Flores-Medina, F. Hernández-Olivares, Influence of fibers partially coated with rubber from tire recycling as aggregate on the acoustical properties of rubberized concrete, Construct. Build. Mater. 129 (2016) 25–36, https://doi.org/10.1016/j.conbuildmat.2016.11.007.
[9] B. Zhang, C.S. Poon, Sound insulation properties of rubberized lightweight aggregate concrete, J. Clean. Prod. 172 (2018) 3176–3185, https://doi.org/10.1016/j.jclepro.2017.11.044.
[10] S. Liu, K. Zhu, S. Cui, X. Shen, G. Tan, Energy & Buildings A novel building material with low thermal conductivity : rapid synthesis of foam concrete reinforced silica aerogel and energy performance simulation, Energy Build. 177 (2018) 385–393, https://doi.org/10.1016/j.enbuild.2018.08.014.
[11] BS:EN 206-1, Concrete – Complementary British Standard to BS EN 206-1. Part 1: Method of Specifying and Guidance for the Specifier, 2012.
[12] P. Sikora, T. Rucinska, D. Stephan, S.Y. Chung, M. Abd Elrahman, Evaluating the effects of nanosilica on the material properties of lightweight and ultra-lightweight concrete using image-based approaches, Construct. Build. Mater. 264 (2020), 120241, https://doi.org/10.1016/j.conbuildmat.2020.120241.
[13] K.C. Thienel, T. Haller, N. Beuntner, Lightweight concrete-from basics to innovations, Materials 13 (2020), https://doi.org/10.3390/ma13051120.
[14] Z.S. Yap, W.C. Liew, N.H.A. Khalid, Z. Haron, A. Mohamed, N.N.A. Rasid, N.Z. Mohammad, Trend of Sound Absorption Research: A Bibliometric Analysis, Civil and Environmental Engineering, 2022, https://doi.org/10.2478/cee-2022-0033, 0.
[15] A. Arora, A. Almujaddidi, F. Kianmofrad, B. Mobasher, Material design of economical ultra-high performance concrete (UHPC) and evaluation of their properties, Cement Concr. Compos. 104 (2019), 103346, https://doi.org/10.1016/j.cemconcomp.2019.103346.
[16] Y. Shi, G. Long, X. Zen, Y. Xie, T. Shang, Design of binder system of eco-efficient UHPC based on physical packing and chemical effect optimization, Construct. Build. Mater. 274 (2021), 121382, https://doi.org/10.1016/j.conbuildmat.2020.121382.
[17] Y. Gowda, T. Girijappa, S.M. Rangappa, Natural fibers as sustainable and renewable resource for development of eco-friendly composites: a comprehensive review. https://doi.org/10.3389/fmats.2019.00226, 2019, 6, 1-14.
[18] H.M. Hamada, A.A. Al-Attar, B. Tayeh, F.B.M. Yahaya, Optimizing the concrete strength of lightweight concrete containing nano palm oil fuel ash and palm oil clinker using response surface method, Case Stud. Constr. Mater. 16 (2022), e01061, https://doi.org/10.1016/j.cscm.2022.e01061.
[19] I.S. Agwa, O.M. Omar, B.A. Tayeh, B.A. Abdelsalam, Effects of using rice straw and cotton stalk ashes on the properties of lightweight self-compacting concrete, Construct. Build. Mater. 235 (2020), 117541, https://doi.org/10.1016/j.conbuildmat.2019.117541.
[20] D. Ba, J. Curpek, M. Cekon, N. Ijaz, Lightweight concrete from a perspective of sustainable reuse of waste byproducts. https://doi.org/10.1016/j.conbuildmat.2021.126061, 2022, 319.
[21] E. Uitterhaegen, L. Labonne, O. Merah, T. Talou, Impact of thermomechanical fiber pre-treatment using twin-screw extrusion on the production and properties of renewable binderless coriander fiberboards. https://doi.org/10.3390/ijms18071539, 2017.
[22] V. Placet, The influence of unintended field retting on the physicochemical and mechanical properties of industrial hemp bast fibres, J. Mater. Sci. 52 (2017) 5759–5777, https://doi.org/10.1007/s10853-017-0811-5.
[23] L. Bleuze, G. Lashermes, G. Alavoine, S. Recous, B. Chabbert, Industrial Crops & Products Tracking the dynamics of hemp dew retting under controlled environmental conditions, Ind. Crop. Prod. 123 (2018) 55–63, https://doi.org/10.1016/j.indcrop.2018.06.054.
[24] M.P. Sáez-pérez, M. Brümmer, J.A. Durán-suárez, Effect of the state of conservation of the hemp used in geopolymer and hydraulic lime concretes. https://doi.org/10.1016/j.conbuildmat.2021.122853, 2021, 285.
[25] C. Lühr, R. Pecenka, J. Budde, T. Ho, H. Gusovius, Comparative investigations of fibreboards resulting from selected hemp varieties, Ind. Crop. Prod. 118 (2018) 81–94, https://doi.org/10.1016/j.indcrop.2018.03.031.
[26] B. Poletanovic, J. Dragas, I. Ignjatovic, M. Komljenovic, I. Merta, Physical and mechanical properties of hemp fibre reinforced alkali-activated fly ash and fly ash/slag mortars, Construct. Build. Mater. 259 (2020), https://doi.org/10.1016/j.conbuildmat.2020.119677, 119677.
[27] T. Jami, S.R. Karade, L.P. Singh, A review of the properties of hemp concrete for green building applications, J. Clean. Prod. 239 (2019), 117852, https://doi.org/10.1016/j.jclepro.2019.117852.
[28] N. Shanmugasundaram, S. Praveenkumar, Influence of supplementary cementitious materials, curing conditions and mixing ratios on fresh and mechanical properties of engineered cementitious composites – a review, Construct. Build. Mater. J. 309 (2021), https://doi.org/10.1016/j.conbuildmat.2021.125038.
[29] N.Z. Mohammad, Y.Z. Shyong, Z. Haron, M. Ismail, A. Mohamed, N.H.A. Khalid, The feasibility of rock wool waste utilisation in a double-layer concrete brick for acoustic: a conceptual review, J. Comput. Theor. Nanosci. 17 (2020) 635–644, https://doi.org/10.1166/jctn.2020.8763.

[30] Z.S. Yap, N.H.A. Khalid, Z. Haron, A. Mohamed, M. Tahir, Waste mineral wool and its opportunities—a review zhen, Materials 14 (2021), https://doi.org/10.3390/ma14195777.
[31] B. Mohammadi, G.M. Amir Ershad-Langroudi, A. Safaiyan, P. Habibi, Mechanical and sound absorption properties of open-cell polyurethane foams modified with rock wool fiber.pdf, J. Build. Eng. 48 (2022), https://doi.org/10.1016/j.jobe.2021.103872.
[32] B. Mohammadi, A. Safaiyan, P. Habibi, G. Moradi, Evaluation of the acoustic performance of polyurethane foams embedded with rock wool fibers at low-frequency range; design and construction, Appl. Acoust. 182 (2021), 108223, https://doi.org/10.1016/j.apacoust.2021.108223.
[33] M.M. Seraji, S. Kianersi, S.H. Hosseini, J. Davarpanah, S. Elahi, Performance evaluation of glass and rock wool fibers to improve thermal stability and mechanical strength of monolithic phenol-formaldehyde based carbon aerogels, J. Non-Cryst. Solids 491 (2018) 89–97, https://doi.org/10.1016/j.jnoncrysol.2018.04.012.
[34] Q. Yan, Z. Meng, J. Luo, Z. Wu, Experimental study on improving the properties of rock wool and glass wool by silica aerogel, Energy Build. 247 (2021), 111146, https://doi.org/10.1016/j.enbuild.2021.111146.
[35] ASTM C567, Standard test method for determining density of structural lightweight concrete, West Conshohocken, PA, https://doi.org/10.1520/C0567, 2004.
[36] ASTM C267, Standard test methods for chemical resistance of mortars, grouts, and monolithic surfacings and polymer concretes, West Conshohocken, PA, https://doi.org/10.1520/C0267-01R06.2, 2006.
[37] BS EN 12390-3, Testing Hardened Concrete Part3: Compressive Strength of Test Specimens, 2009.
[38] ASTM C496, ASTM C496-11 standard test method for splitting tensile strength of cylindrical concrete specimens, West Conshohocken, PA, https://doi.org/10.1520/C0496, 2011.
[39] C.78 ASTM, Standard test method for flexural strength of concrete (using simple beam with third-point loading), West Conshohocken, PA, https://doi.org/10.1520/C0078-02, 2002.
[40] A.B. Moradikhou, A. Esparham, M. Jamshidi Avanaki, Physical & mechanical properties of fiber reinforced metakaolin-based geopolymer concrete, Construct. Build. Mater. 251 (2020), https://doi.org/10.1016/j.conbuildmat.2020.118965, 118965.
[41] O. Olofinnade, S. Chandra, P. Chakraborty, Recycling of high impact polystyrene and low-density polyethylene plastic wastes in lightweight based concrete for sustainable construction, Mater. Today Proc. 38 (2020) 2151–2156, https://doi.org/10.1016/j.matpr.2020.05.176.
[42] Z.C. Muda, P. Shafigh, N.B. Mahyuddin, S.M.E. Sepasgozar, S. Beddu, A. Zakaria, Energy performance of a high-rise residential building using fibre-reinforced structural lightweight aggregate concrete, Appl. Sci. (2020) 10, https://doi.org/10.3390/app10134489.
[43] M. Amran, R. Fediuk, H.S. Abdelgader, G. Murali, T. Ozbakkaloglu, Y.H. Lee, Y.Y. Lee, Fiber-reinforced alkali-activated concrete: a review, J. Build. Eng. 45 (2022), 103638, https://doi.org/10.1016/j.jobe.2021.103638.
[44] V. Jarugumalli, L.N.K.S. Madupu, Study on properties of porous concrete incorporating aloevera and marble waste powder as a partial cement replacement, Mater. Today Proc. (2022), https://doi.org/10.1016/j.matpr.2021.11.595.
[45] H. Xiong, K. Yuan, J. Xu, M. Wen, Pore structure, adsorption, and water absorption of expanded perlite mortar in external thermal insulation composite system during aging, Cement Concr. Compos. 116 (2021), 103900, https://doi.org/10.1016/j.cemconcomp.2020.103900.
[46] D. Shen, C. Wen, P. Zhu, Y. Wu, Y. Wu, Influence of Barchip fiber on early-age autogenous shrinkage of high-strength concrete internally cured with super absorbent polymers, Construct. Build. Mater. 264 (2020), https://doi.org/10.1016/j.conbuildmat.2020.119983, 119983.
[47] R. Dávila-Pompermayer, L.G. Lopez-Yepez, P. Valdez-Tamez, C.A. Juárez, A. Durán-Herrera, Lechugilla natural fiber as internal curing agent in self compacting concrete (SCC): mechanical properties, shrinkage and durability, Cement Concr. Compos. 112 (2020), https://doi.org/10.1016/j.cemconcomp.2020.103686.
[48] D. Shen, C. Liu, C. Li, X. Zhao, G. Jiang, Influence of Barchip fiber length on early-age behavior and cracking resistance of concrete internally cured with super absorbent polymers, Construct. Build. Mater. 214 (2019) 219–231, https://doi.org/10.1016/j.conbuildmat.2019.03.209.
[49] D. Shen, Z. Feng, J. Kang, C. Wen, H. Shi, Effect of Barchip fiber on stress relaxation and cracking potential of concrete internally cured with super absorbent polymers, Construct. Build. Mater. 249 (2020), 118392, https://doi.org/10.1016/j.conbuildmat.2020.118392.
[50] G. Ren, B. Yao, M. Ren, X. Gao, Utilization of natural sisal fibers to manufacture eco-friendly ultra-high performance concrete with low autogenous shrinkage, J. Clean. Prod. 332 (2022), 130105, https://doi.org/10.1016/j.jclepro.2021.130105.
[51] M. Amin, B.A. Tayeh, I. saad agwa, Investigating the mechanical and microstructure properties of fibre-reinforced lightweight concrete under elevated temperatures, Case Stud. Constr. Mater. 13 (2020), e00459, https://doi.org/10.1016/j.cscm.2020.e00459.
[52] L. Wang, F. Aslani, I. Hajirasouliha, E. Roquino, Ultra-lightweight engineered cementitious composite using waste recycled hollow glass microspheres, J. Clean. Prod. 249 (2020), https://doi.org/10.1016/j.jclepro.2019.119331, 119331.
[53] F. Aslani, A. Dehghani, L. Wang, The effect of hollow glass microspheres, carbon nanofibers and activated carbon powder on mechanical and dry shrinkage performance of ultra-lightweight engineered cementitious composites, Construct. Build. Mater. 280 (2021), 122415, https://doi.org/10.1016/j.conbuildmat.2021.122415.
[54] K. Srinivas, K.R. Akula, V. Mahesh, Experimental investigation on lightweight concrete by replacing the coarse aggregate with coconut shell and expanded polystyene beads and using polypropylene fiber, Mater. Today Proc. 46 (2021) 838–842, https://doi.org/10.1016/j.matpr.2020.12.834.
[55] ASTM C330, Standard Specification for Lightweight Aggregates for Structural Concrete, 2009. West Conshohocken, PA.
[56] MS76, Specifications for Bricks and Blocks of Fired Bricks, Clay or Shale, 1972. Part 2.
[57] D. Altalabani, D.K.H. Bzeni, S. Linsel, Mechanical properties and load deflection relationship of polypropylene fiber reinforced self-compacting lightweight concrete, Construct. Build. Mater. 252 (2020), https://doi.org/10.1016/j.conbuildmat.2020.119084, 119084.
[58] B. Zhang, Y. Feng, J. Xie, J. He, Y. Zhang, C. Cai, D. Huang, L. Li, Effects of fibres on ultra-lightweight high strength concrete: dynamic behaviour and microstructures, Cement Concr. Compos. 128 (2022), 104417, https://doi.org/10.1016/j.cemconcomp.2022.104417.
[59] Y. Zeng, X. Zhou, A. Tang, Shear performance of fibers-reinforced lightweight aggregate concrete produced with industrial waste ceramsite-Lytag after freeze-thaw action, J. Clean. Prod. 328 (2021), 129626, https://doi.org/10.1016/j.jclepro.2021.129626.
[60] I.A. Wani, R. ul Rehman Kumar, Experimental investigation on using sheep wool as fiber reinforcement in concrete giving increment in overall strength, Mater. Today Proc. 45 (2021) 4405–4409, https://doi.org/10.1016/j.matpr.2020.11.938.
[61] ACI 318, Building Code Requirements for Structural Concrete, 2014.
[62] Y.H.M. Amran, N. Farzadnia, A.A.A. Ali, Properties and applications of foamed concrete; A review, Construct. Build. Mater. 101 (2015) 990–1005, https://doi.org/10.1016/j.conbuildmat.2015.10.112.
[63] D.S. Babu, K. Ganesh Babu, T.H. Wee, Properties of lightweight expanded polystyrene aggregate concretes containing fly ash, Cement Concr. Res. 35 (2005) 1218–1223, https://doi.org/10.1016/j.cemconres.2004.11.015.
[64] M. Gesoglu, T. Özturan, E. Güneyisi, Shrinkage cracking of lightweight concrete made with cold-bonded fly ash aggregates, Cement Concr. Res. 34 (2004) 1121–1130, https://doi.org/10.1016/j.cemconres.2003.11.024.
[65] T.Z.H. Ting, M.E. Rahman, H.H. Lau, M.Z.Y. Ting, Recent development and perspective of lightweight aggregates based self-compacting concrete, Construct. Build. Mater. 201 (2019) 763–777, https://doi.org/10.1016/j.conbuildmat.2018.12.128.
[66] Y. Choi, M.-M. Kang, The relationship between splitting tensile strength and compressive strength of fiber reinforced concretes, J. Korea Concr. Inst. 15 (2003) 155–161, https://doi.org/10.4334/jkci.2003.15.1.155.
[67] N. Narayanan, K. Ramamurthy, Structure and properties of aerated concrete: a review, Cement Concr. Compos. 22 (2000) 321–329, https://doi.org/10.1016/S0958-9465(00)00016-0.
[68] R. Chen, S. Ahmari, L. Zhang, Utilization of sweet sorghum fiber to reinforce fly ash-based geopolymer, J. Mater. Sci. 49 (2014) 2548–2558, https://doi.org/10.1007/s10853-013-7950-0.
[69] O. Gencel, O. Yavuz Bayraktar, G. Kaplan, A. Benli, G. Martínez-Barrera, W. Brostow, M. Tek, B. Bodur, Characteristics of hemp fibre reinforced foam concretes with fly ash and Taguchi optimization, Construct. Build. Mater. 294 (2021), 123607, https://doi.org/10.1016/j.conbuildmat.2021.123607.